Title	Perpendicular orientation between dispersed rubber and polypropylene molecules in an oriented sheet
Author(s)	Phulkerd, Panitha; Funahashi, Yoshiaki; Ito, Asae; Iwasaki, Shohei; Yamaguchi, Masayuki
Citation	Polymer Journal, 50: 309-318
Issue Date	2018-01-23
Type	Journal Article
Text version	author
URL	http://hdl.handle.net/10119/16124
Rights	This is the author-created version of Springer, Panitha Phulkerd, Yoshiaki Funahashi, Asae Ito, Shohei Iwasaki, Masayuki Yamaguchi, Polymer Journal, 50, 2018, 309-318. The original publication is available at www.springerlink.com, http://dx.doi.org/10.1038/s41428-017-0017-3
Description	

Perpendicular Orientation of Dispersed Rubber in an Oriented Polypropylene Sheet

Panitha Phulkerd[1]*, Yoshiaki Funahashi[1], Shohei Iwasaki[2], and

Masayuki Yamaguchi[1]

[1]School of Materials Science,

Japan Advanced Institute of Science and Technology

1-1 Asahidai, Nomi, Ishikawa 923-1292, JAPAN

[2] New Japan Chemical Co., Ltd.,

13 Yoshijima, Yaguracho, Fushimi, Kyoto 612-8224, JAPAN

_____

* Corresponding author:
Panitha Phulkerd
School of Materials Science, Japan Advanced Institute of Science and Technology,
1-1 Asahidai, Nomi, Ishikawa 923-1292, Japan
Phone: +81-761-51-1623; Fax: +81-761-51-1149;
E-mail: panitha@jaist.ac.jp

26 Abstract

27   An immiscible blend of isotactic polypropylene (PP) and ethylene-butene-1

28 copolymer (EB) (PP/EB = 70/30) containing a small amount of *N,N'*-dicyclohexyl-2,6-

29 naphthalenedicarboxamide as a nucleating agent for β-form crystals was prepared by T-

30 die extrusion. We successfully prepared an extruded sheet, in which the orientation of the

31 PP molecules is perpendicular to the deformation of the EB particles; i.e., the β-form

32 crystals of PP are predominantly oriented perpendicular to the flow direction of the sheet

33 plane (the transverse direction, TD), whereas the EB droplets are strongly deformed in

34 the flow direction. It should be noted that the EB barely affects the crystalline form and

35 orientation of PP. This extraordinary structure provides unique mechanical anisotropy.

36 The tear strength in the TD sample is significantly enhanced with the anomalous crack

37 propagation in the machine direction (MD). Moreover, the anisotropy in tensile properties

38 such as Young's modulus, yield stress, strain at break, and dynamic tensile modulus

39 becomes reduced.

40

43

44

45

46

47

48

49

Introduction

Isotactic polypropylene (PP) is widely used in various applications because it is inexpensive and lightweight. In particular, the trend in the automobile industry to use PP will continue because weight reduction is an inevitable future priority. Generally speaking, both rigidity and high impact strength are required for a material design of PP [1]. Therefore, the technology of the blend with rubber [1-17] and fillers [18,19] and the addition of a nucleating agent [20-25] has been intensively studied. Various types of elastomeric materials have been employed as impact modifiers. In particular, after the development of metallocene catalyst, ethylene-butene-1, ethylene-hexene-1, and ethylene-octene-1 copolymers have been preferred for this purpose, because they have low interfacial tension with PP compared with traditional ethylene-propylene copolymers. Such miscibility and/or compatibility have been predicted by the difference in statistical segment length [1,12,17] and packing length [8,14,17], and have been summarized from the perspective of the species and content of the α-olefin [2,3,7,15]. The rheological properties [4,5,9], crystallization behavior [6,16], and processability [10,11] of PP blends with ethylene-α-olefin copolymers have also been elucidated. Accordingly, controlling the particle size of a rubber dispersion in a PP continuous phase improves the mechanical properties of the material. In general, low interfacial tension, and viscosity matching between components enable the formation of small particles with uniform dispersion by melt blending. Furthermore, the nucleation process of PP plays a key role in the processing operation because its mechanical properties are largely dependent on the form and degree of crystallinity. As well known, PP has various crystalline forms such as monoclinic α modification, trigonal β modification, orthorhombic γ modification, and

74 smectic form, which are determined by crystallization conditions and additives

75 [2,3,7,8,12,14,17]. Of all the crystalline structures, recent attention has focused on β-form

76 crystals owing to the development of highly efficient nucleating agents such as 1,3,5-

77 benzenetrisamide [26] and *N,N'*-dicyclohexyl-2,6-naphthalenedicarboxamide [27,28].

78 These nucleating agents enhance the modulus, which was considered one of the

79 unfavorable properties of β-form crystals. Moreover, a recent report on the enhancement

80 of the melting point using β-form crystals [29] should encourage the industrial

81 applications.

82   *N,N'*-dicyclohexyl-2,6-naphthalenedicarboxamide has been used to ensure the

83 molecular orientation of the PP chains in the transverse direction (TD) [30-35]. Under

84 suitable processing conditions, the nucleating agent appears as needle-shaped crystals in

85 PP, and is aligned with the direction of flow by hydrodynamic force. Owing to the unique

86 crystallization behavior of PP, in which the *c*-axis of the PP crystals grows perpendicular

87 to the long axis of the needle-shaped nucleating agent by epitaxial crystallization, the PP

88 chains orient perpendicular to the flow direction during T-die extrusion [31]. The resulting

89 product has unique mechanical properties. Orientation control using nucleating agents is

90 applicable to injection-molding. The peculiar orientation of the PP chains, i.e., in a

91 plywood-like structure, prohibits crack propagation and reduces anisotropy in modulus

92 and in thermal expansion [32,35]. A combined approach involving the addition of rubber

93 and the control of orientation using a specific β nucleating agent is expected to maximize

94 the mechanical performance of PP. Although several papers have been published

95 regarding polymer blends of PP and ethylene-α-olefin copolymers, there have been few

96 reports describing in detail of PP blends containing a β nucleating agent [36-39].

97 Furthermore, in industrial applications the molecular orientation of the PP and the rubber

98 dispersion are controlled independently.

99   The present research focuses on an extruded sheet comprising PP and ethylene-

100 butene-1 copolymer (EB) with the nucleating agent, N,N'-dicyclohexyl-2,6-naphthalene-

101 dicarboxamide. The orientation of the PP molecular chains and the deformation direction

102 of the rubber particles are investigated in detail with an evaluation of the mechanical

103 properties.

104

105   **Materials and Methods**

106

107 Materials

108   The raw materials used in the present study were: a commercially available

109 isotactic polypropylene homopolymer (PP) (SunAllomer, PM600A, melt flow rate (MFR)

110 7.5 [g/10 min at 230°C], Mn 63,000, Mw 360,000), and an ethylene-butene-1 copolymer

111 (EB) (Mitsui Chemicals, TAFER DF610, MFR 2.2 [g/10 min at 230°C], density 860

112 kg/m^3, ethylene content 54 wt.%). N,N'-dicyclohexyl-2,6-naphthalenedicarboxamide

113 (New Japan Chemical, NJ Star NU-100) was used as a β nucleating agent without further

114 purification.

115

116 Sample preparation

117   Melt-mixing of PP with 0.1 wt.% of the β nucleating agent was performed by a

118 counter-rotating twin-screw extruder (Technovel, KZW15TW-45MG-NH) with 0.05

119 wt.% of 3-(3,5-di-tert-butyl-4-hydroxyphenyl)propionate (Ciba, Irganox 1010) and 0.1

120 wt.% of tris(2,4-di-tert-butyl-phenyl)phosphate (Ciba, Irgafos 168) as thermal stabilizers,

121 and 0.05 wt.% of calcium stearate (Nitto Kasei Kogyo) as a neutralizing agent. The screw

122 diameter of the extruder was 15 mm and the length-to-diameter ratio was 45. The machine

123 was operated at a screw rotation speed of 250 rpm. The mixing was performed at 260°C

124 to completely dissolve the nucleating agent in molten PP. The extruded strands were

125 dipped in a water-bath and cut into pellets approximately 2.3 mm in diameter.

126   The pellets of PP containing the nucleating agent and EB were fed into a single-

127 screw extruder (Technovel, SZW25GT-28VG-STD) equipped with a T-die (300 mm wide

128 with a 0.5 mm die lip) at a blend ratio of 70/30 (PP/EB) by weight. The out-put rate was

129 3 kg/h. The screw diameter and the length-to-diameter ratio were 25 mm and 28,

130 respectively. The speed of screw rotation was 40 rpm. The sheet was stretched in the air

131 gap (10 mm) between the die lip and the chill roll. The temperatures of the die and chill

132 roll were maintained at 200°C and 103°C, respectively. The diameter of the chill roll was

133 250 mm and the rotational speed was 1 rpm. Reference samples comprising extruded

134 sheets of PP containing the nucleating agent and PP/EB without the nucleating agent were

135 also prepared under conditions identical to those described above.

136

137 Measurements

138   Thermal analysis was conducted using a differential scanning calorimeter (DSC)

139 (Perkin Elmer, DSC 8000) under a nitrogen atmosphere to avoid thermal-oxidative

140 degradation. Samples weighing approximately 3 mg were sealed in aluminum pans. The

141 melting and crystallization profiles were recorded at a heating rate of 10°C min^{-1} and a

142 cooling rate of 10°C min^{-1}.

143   The temperature dependence of the dynamic tensile moduli of the extruded

144 sheets was measured between -80°C and 175°C using a dynamic mechanical analyzer

145 (UBM, Rheologel-E4000-DVE). The frequency was 10 Hz and the heating rate was 2°C

146 min^{-1}. The extruded sheet was cut into small rectangular pieces, 5 mm wide and 20 mm

147 long, that were mounted between gauges with a distance of 10 mm. The measurements

148 were carried out on two types of sample to investigate the mechanical anisotropy: one

149 was cut parallel to the flow direction (the machine direction (MD) sample), and the other

150 was perpendicular to the flow direction (the transverse direction (TD) sample). In the case

151 of the MD sample, the direction of the applied oscillatory strain coincided with the flow

152 direction.

153   To analyze the orientation and crystalline form of the PP molecules, wide-angle

154 X-ray diffraction (WAXD) patterns were collected using a high-speed two-dimensional

155 X-ray detector (Rigaku, PILATUS 3R 100K). The measurements were carried out using

156 CuKα radiation operated at 40 kV and 30 mA with a scanning range of 2θ (the Bragg

157 angle) from 10° to 30°. Small pieces of the sample (approximately 1.0 mm thick) were

158 mounted on the diffractometer. The X-ray beam was irradiated normal to the MD-ND

159 plane (edge view: EV) and the MD-TD plane (through view: TV). For the EV

160 measurements, ten sheets of the sample were laminated with polystyrene solution,

161 whereas only one sheet was used for the TV measurements.

162   The orientation of the PP lamellae was investigated using a transmission electron

163 microscopy (TEM) (JEOL, JEM-2100FX) at an acceleration voltage of 200 kV. The

164 samples were embedded in epoxy resin and sectioned using an ultramicrotome (RMC-

165 Boeckeler, Ultramicrotome MT-XL) equipped with a diamond knife after exposure to the

166 vapor of ruthenium tetraoxide at 40°C for a day. Cross-sectional specimens (100 nm

167 thick) were cut from the stained sample in the MD-ND plane.

168   The deformation of the EB dispersed phase was observed by means of a scanning

169   electron microscopy (SEM) (Hitachi, S4100) with an acceleration voltage of 20 kV. For

170   non-conductive samples, the specimens were coated with Pt/Pd alloy for 60 seconds by

171   an ion sputtering machine (Hitachi, E1010). The surface of specimen was removed using

172   a rotary microtome (Yamato Kohki Industrial, RX-860) and immersed in xylene at room

173   temperature for 3 days to elute the rubber particles.

174   Stress-strain curves were investigated at room temperature using a tensile

175   machine (Tokyo Testing Machine, LSC-05/300) following ASTM D638. The specimens

176   were cut into dumbbell-shaped pieces (10 mm wide and 40 mm long) using dumbbell

177   cutter No.3 referenced from JIS K6251, in which the sample size was reduced by 40%.

178   The initial distance between the gauges was 30 mm, and one of the crossheads was moved

179   up at a constant speed of 10 mm min^{-1}. Stretching was performed in two directions: one

180   was parallel to the flow direction (the machine direction (MD) sample) and the other was

181   perpendicular to the flow direction (the transverse direction (TD) sample). All

182   measurements were performed at least five times, and the average values were calculated.

183   The elongation at break was evaluated by measuring the final gauge length of the narrow

184   part of the dumbbell.

185   The tear test was investigated by the Trouser method using a tensile machine

186   (Tokyo Testing Machine, LSC-05/300). Two types of sample were cut from the extruded

187   sheet; one had a notch parallel to the flow direction, that is, the machine direction (MD),

188   and the other had a vertical notch, that is, the transverse direction (TD). The specimens

189   were stretched at room temperature at a speed of 200 mm min^{-1}. The distance between

190   the gauges was 20 mm.

191

192   **Results and Discussion**

193

194   Characterization of blend sheets

195   The melting and crystallization behaviors of the extruded sheets are shown in

196   Fig. 1. As shown in Fig. 1a, the pure PP sheet exhibits a main melting peak at 165°C,

197   suggesting α-form crystals with a small shoulder peak of β-form crystals at 150°C. A

198   similar melting profile is observed in the PP/EB sheet. For the sheet containing the

199   nucleating agent, two distinct peaks are detected at 145°C and 151°C, which can be

200   attributed to β-form crystals. Furthermore, a sharp peak due to the α-form crystals appears

201   at a slightly higher temperature than that for pure PP. The recrystallization after melting

202   of thick β-form crystals is responsible for thick lamellae of α-form crystals leading to the

203   enhanced melting point as explained by Phulkerd et al. [29]. The same phenomenon is

204   observed for the PP/EB sheet containing the nucleating agent. Under suitable cooling

205   conditions, an annealed sheet of PP containing the nucleating agent has a melting point

206   due to α-form crystals nearly at 170°C [29].

207   The crystallization behavior during the cooling process from 200°C is shown in

208   Fig. 1b. There is no significant difference in the exothermic crystallization temperature

209   (ca. 117°C) between the pure PP and PP/EB sheets. After the addition of the nucleating

210   agent, the crystallization peak shifts to a higher temperature at 128°C in both the PP and

211   PP/EB sheets. In this experiment, the crystallization temperature of PP is barely affected

212   by EB irrespective of the addition of the nucleating agent, which also indicates that EB

213   particles hardly affect the nucleating ability of the nucleating agent.

214

215   [Fig. 1]

216   Fig. 2 shows the X-ray diffraction curves in the equatorial direction of the MD-

217   TD plane, which are transformed and corrected using Lorentz and polarization (Lp)

218   factors. Both α- and β-form crystals are detected but the β-form crystals are predominant

219   in the sheets containing the nucleating agent. In the sheets without the nucleating agent,

220   the strong peak ascribed to the α-form crystals are detected, although β(110) and β(111)

221   peaks are still confirmed. Relatively high cooling temperature (the chill roll was

222   maintained at 103°C) induces the β-form crystallization to some extent. The XRD

223   patterns also suggest that the addition of EB to PP has a negligible effect on crystal

224   formation. Furthermore, there is an indication that the crystallinity of EB is significantly

225   low in the extruded sheets, because both (110) and (200) planes, which are attributable to

226   polyethylene crystals, are absent.

227

228   [Fig. 2]

229

230   Fig. 3 shows the 2D-WAXD patterns of the extruded sheets, obtained by

231   directing the X-ray beam in the normal direction for the edge view and in the transverse

232   direction for the through view. The α-form crystals in the pure PP show weak orientation,

233   as seen in Fig. 3a. The diffraction patterns of the PP/EB sheet (Fig. 3b) are almost

234   identical to those of the PP sheet, in which a diffraction peak attributed to the (040) plane

235   of the α-form crystals is detected in the equatorial direction, demonstrating that the PP

236   molecular chains are oriented in the MD direction. For the PP sheet containing the

237   nucleating agent (Fig. 3c), the PP chains in the β-form crystals were oriented in the TD

238   direction. Such molecular orientation is also detected in the PP/EB sheet containing the

239   nucleating agent, in which distinct arcs ascribed to (110) reflection of the β-form crystals

240   are observed as shown in Fig. 3d. This result demonstrates that PP chains preferentially

241   orient perpendicular to the flow direction. It also indicates that the nucleating agent

242   promotes the growth of β-form crystals with the TD orientation of the PP molecular chains,

243   irrespective of the presence of EB.

244

245   [Fig. 3]

246

247   Fig. 4 shows a TEM image of a thin slice of the TD-ND plane cut from the PP/EB

248   sheet containing the nucleating agent. Phase-separated morphology is clearly seen in this

249   sample, in which the dark region is the EB phase. Furthermore, the crystalline lamellae

250   of PP are detected in the matrix as white lines, which preferentially orient along the ND.

251   Therefore, the growth direction of the PP chains is perpendicular to the ND, i.e., the TD

252   orientation, which corresponds well with the XRD patterns. The compressed stress

253   applied during the chill roll process is responsible for the preferential TD orientation of

254   PP chains, not the ND orientation. The slight deformation of EB particles to the TD would

255   be also attributed to the compression stress at the chill roll, although the deformation of

256   EB particles will be explained in detail later. Furthermore, PP lamellae are incorporated

257   into EB phase, which will provide the strong adhesion between them. This phenomenon

258   is attributed to the low interfacial tension between PP and EB, leading to large interphase

259   thickness in the molten state.

260

261   [Fig. 4]

262

263   Fig. 5 shows SEM images for the PP/EB sheet containing the nucleating agent.

264   The dark regions are attributable to the elongated pores formed by elution of the EB

265   particles with xylene. As seen in Fig. 5a, the numerous pores are mainly deformed in the

266   flow direction. The length of the pores is found to be approximately 3.0 μm and the

267   diameter is about 0.5 μm. On the other hand, a slight deformation in the TD direction with

268   an averaged pore size of 1.0 μm for the length and 0.5 μm for the diameter is detected in

269   the TD-ND plane, owing to the pressure applied by the chill roll, which corresponds with

270   the TEM image. The marked difference in the pore size between the MD and TD

271   directions demonstrates that EB preferentially orients in the flow direction. This is

272   understandable because the elongational stress in the air gap as well as the shear stress in

273   the die deform the EB particles in the flow direction by the hydrodynamic force. Similar

274   SEM images were obtained for the PP/EB sheet without the nucleating agent (but they

275   are not presented here). This suggests that the nucleating agent hardly affects the rubber

276   dispersion and deformation.

277

278   [Fig. 5]

279

280   Mechanical properties

281   Because the molecular orientation of PP is different from that of EB, the sample

282   sheet exhibits anomalous mechanical properties. Fig. 6 shows the dynamic mechanical

283   properties of extruded sheets employing two specimens to apply the oscillatory stain in

284   the different directions, i.e., the machine direction (MD) and transverse direction (TD).

285   As seen in Fig. 6a, both the MD and TD samples for the pure PP sheet show almost the

286   same dynamic tensile moduli over the whole range of temperature. A similar behavior is

287   also detected in the PP/EB sheet, in which PP molecules orient to the flow direction. Since

288   the molecular orientation is weak, no obvious mechanical anisotropy is observed for the

289   sample sheets without the nucleating agent. Moreover, E' in PP/EB falls off markedly

290   around 165°C which is attributed to melting of α-form crystals. For the PP sheet

291   containing the nucleating agent, in contrast, E' in TD is higher than that in MD at low

292   temperatures and vice versa at high temperatures. Based on the mechanical model

293   proposed by Takayanagi et al. [40], the anisotropy of the tie chain fractions, which are

294   deformed in the flow direction by hydrodynamic force during extrusion, is responsible

295   for the crossing behavior in the sample containing the nucleating agent [33]. A similar

296   mechanical behavior is detected for the PP/EB sheet containing the nucleating agent,

297   albeit the crossing behavior is weaker and shifted to the lower temperature region. As

298   compared with the PP/EB sheet, the addition of the nucleating agent enhances E' for the

299   MD sample over a wide temperature range above the glass transition (T_g), owing to a high

300   degree of crystallinity resulting from the nucleating effect. Furthermore, a sharp drop of

301   E' is detected around 150°C due to the melting of the β-form crystals, which corresponds

302   to the DSC and WAXD results. It is found from Fig. 6b that both the PP/EB sheets with

303   or without the nucleating agent exhibit double peaks in the E'' curve in the temperature

304   range from -75°C to 40°C; the peak at the higher temperature is attributed to T_g of PP and

305   the other at the lower one is to that of EB.

306

307   [Fig. 6]

308

309   The stress-strain curves at the strain rate of 0.006 s^{-1} are shown in Fig. 7. The

310   tensile force is applied along the MD or the TD. The difference in the tensile behavior

311   between stretching in the MD and TD is detected in all samples. As seen in Fig. 7a, the

312   pure PP sheet experiences a brittle fracture in the TD stretching beyond the yield point.

313   In the case of MD stretching, however, ductile deformation occurs under a low yield

314   stress. The PP containing the nucleating agent (Fig. 7b) shows high Young's modulus,

315   which corresponds to the tensile storage modulus. Moreover, yield stress in the MD

316   stretching is greatly enhanced with a ductile manner. The low modulus of EB is

317   responsible for marked decrease in Young's modulus and yield stress for both the PP/EB

318   and PP/EB containing the nucleating agent as seen in Figs. 7c and 7d. In the PP/EB sheet

319   containing the nucleating agent, the anisotropy in Young's modulus and yield stress is

320   considerably weaker than that in the PP sheet containing the nucleating agent. The strain

321   at break in the TD stretching for PP containing the nucleating agent is considerably larger

322   than that for pure PP. The ductile behavior is also observed in MD stretching, although

323   the yield stress is high. As a result, the anisotropy of strain at break becomes reduced

324   following the addition of the nucleating agent. The reduction of the mechanical anisotropy

325   becomes more apparent for the blend containing EB, although it is interesting to note that

326   the PP/EB exhibits ductile behavior not only in MD but also in TD stretching. Since the

327   yield stress in TD stretching is lower than that in MD stretching, the deformation of EB

328   particles into flow direction affects the stress-strain behavior greatly, although the

329   deformation behavior of the EB phase is not revealed in this study. The details of

330   mechanical anisotropy in terms of crack propagation are discussed below.

331

332   [Fig. 7]

333

334   Trouser tear test was carried out at room temperature employing two types of the

335   sheet samples; one has a parallel notch in the flow direction (MD), and the other has a

336   vertical notch (TD). As seen in Fig. 8a, the pure PP sheet shows higher tear strength in

337   the TD sample. For PP containing the nucleating agent (Fig. 8b), the order is opposite

338   with an enhanced anisotropy in tear strength. In the case of the blend, the tear strength in

339   the TD sample is markedly enhanced, irrespective of the nucleating agent. Furthermore,

340   the direction of crack propagation changes to the MD immediately after the stretching as

341   demonstrated in Figs. 8c and 8d. These results demonstrate that PP orientation has no

342   marked impact on the tear property. The deformation of EB particles plays a dominant

343   role on the tearing. Such information has never been reported before to the best of our

344   knowledge, because the deformation direction of a dispersion is always the same as the

345   molecular orientation direction of matrix in general. Regarding the effect of the nucleating

346   agent, the tear strength of the MD sample is slightly enhanced, although the effect is not

347   as obvious as in the pure PP.

348

349   [Fig. 8]

350

351

352   **Conclusions**

353

354   An extruded sheet with unique structure was developed using a blend comprising

355   PP, EB, and a small amount of *N,N'*-dicyclohexyl-2,6-naphthalenedicarboxamide. It was

356   found that the nucleating agent promotes the formation of β-form crystals and causes the

357   PP chains orient perpendicular to the flow direction in an extruded sheet, i.e., in the

358   transverse direction, as confirmed by 2D-XRD and TEM characterization. On the contrary,

359   EB is deformed in the flow direction, as revealed by SEM images. As a result, the chain

360   orientation of the PP molecules is perpendicular to the deformation direction of the EB

361   droplets, which affects the mechanical anisotropy to a great extent. With regard to the

362   tensile properties, the anisotropy in yield stress and strain at break is significantly

363   decreased owing to this peculiar structure. It is proved by the tear test that the strength of

364   the TD sample is increased with a crack growth in the flow direction. This result

365   demonstrates that the deformation of the EB particles in the MD direction exhibits more

366   pronounced effect than the molecular orientation of the PP chains in the TD direction.

367

368   **References**

369

370   1. F.S. Bates, G.H. Fredrickson, Conformational asymmetry and polymer-polymer

371   thermodynamics, Macromolecules 27 (1994) 1065-1067.

372   2. M. Yamaguchi, H. Miyata, K-H Nitta, Compatibility of binary blends of

373   polypropylene with ethylene-α-olefin copolymer, J. Appl. Polym. Sci. 62 (1996) 87-

374   97.

375   3. P.A. Weimann, T.D. Jones, M.A. Hillmyer, F.S. Bates, J.D. Londono, Y. Melnichenko,

376   G.D. Wignall, K. Almdal, Phase behavior of isotactic polypropylene-

377   poly(ethylene/ethylethylene) random copolymer blends, Macromolecules 30 (1997)

378   3650-3657.

379   4. C.J. Carriere, H.C. Silvis, The effects of short-chain branching and comonomer type

380   on the interfacial tension of polypropylene-polyolefin elastomer blends, J. Appl.

381   Polym. Sci. 66 (1997) 1175-1181.

382 5. M. Yamaguchi, K-H Nitta, H. Miyata, T. Masuda, Rheological properties for binary

383   blends of i-PP and ethylene-1-hexene copolymer, J. Appl. Polym. Sci. 63 (1997) 467-

384   474.

385 6. M. Yamaguchi, H. Miyata, K-H Nitta, Structure and properties for binary blends of

386   isotactic polypropylene with ethylene-α-olefin copolymer. 1. Crystallization and

387   morphology, J. Polym. Sci. B Polym. Phys. 35 (1997) 953-961.

388 7. Y. Thomann, J. Suhm, R. Thomann, G. Bar, R.D. Maier, R. Mülhaupt, Investigation of

389   morphologies of one- and two-phase blends of isotactic poly(propene) with random

390   poly(ethene-co-1-butene), Macromolecules 31 (1998) 5441-5449.

391 8. D.J. Lohse, W.W. Graessley, Thermodynamics of polyolefin blends, in: D.R. Paul,

392   C.B. Bucknall (Eds.), Polymer Blends, John Wiley & Sons Inc., New York, 1999, pp.

393   219-237.

394 9. M. Yamaguchi, H. Miyata, Influence of stereoregularity of polypropylene on

395   miscibility with ethylene-1-hexene copolymer, Macromolecules 32 (1999) 5911-5916.

396 10. M. Yamaguchi, K-I Suzuki, H. Miyata, Structure and mechanical properties for binary

397   blends of polypropylene and ethylene-1-hexene copolymer, J. Polym. Sci. B Polym.

398   Phys. 37 (1999) 701-713.

399 11. E.L. Bedia, S. Murakami, K. Senoo, S. Kohjiya, Polymer 43 (2002) 749-755.

400 12. T.D. Jones, K.A. Chaffin, F.S. Bates, Effect of tacticity on coil dimensions and

401   thermodynamic properties of polypropylene, Macromolecules 35 (2002) 5061-5068.

402 13. N. Pasquini, Polypropylene Handbook, second ed., Hanser, Munich, 2005.

403 14. D.J. Lohse, The Influence of chemical structure on polyolefin melt rheology and

404   miscibility, J. Macromol. Sci. Polymer. Rev. 45 (2005) 289-308.

405   15. M. Yamaguchi, Morphology and mechanical properties in iPP/polyolefin-based
406   copolymer blends, in: D. Nwabunma, T. Kyu (Eds.), Polyolefin Blends, John Wiley &
407   Sons Inc., New Jersey, 2008, pp. 224-268.

408   16. J. Yang, J.L. White, Crystallization behavior of polypropylene/ethylene butene
409   copolymer blends, J. Appl. Polym. Sci. 126 (2012) 2049-2058.

410   17. J. Xu, V. Mittal, F.S. Bates, Toughened isotactic polypropylene: Phase behavior and
411   mechanical properties of blends with strategically designed random copolymer
412   modifiers, Macromolecules 49 (2016) 6497-6506.

413   18. Y. Lin, H. Chen, C-M Chan, J. Wu, High impact toughness polypropylene/CaCO$_3$
414   nanocomposites and the toughening mechanism, Macromolecules 41 (2008) 9204-
415   9213.

416   19. R. Wiwattananukul, B. Fan, M. Yamaguchi, Improvement of rigidity for rubber-
417   toughened polypropylene via localization of carbon nanotubes, Comp. Sci. Technol.
418   141 (2017) 106-112.

419   20. Y. Feng, X. Jin, J.N. Hay, Effect of nucleating agent addition on crystallization of
420   isotactic polypropylene, J. Appl. Polym. Sci. 69 (1998) 2089-2095.

421   21. J. Varga, I. Mudra, G.W. Ehrenstein, Highly active thermally stable β-nucleating
422   agents for isotactic polypropylene, J. Appl. Polym. Sci. 74 (1999) 2357-2368.

423   22. G-S Jang, W-J Cho, C-S Ha, Crystallization behavior of polypropylene with or without
424   sodium benzoate as a nucleating agent, J. Polym. Sci. B Polym. Phys. 39 (2001) 1001-
425   1016.

426   23. C. Marco, M.A. Gomez, G. Ellis, J.M. Arribas, Activity of a β-nucleating agent for
427   isotactic polypropylene and its influence on polymorphic transitions, J. Appl. Polym.
428   Sci. 86 (2002) 531-539.

429   24. P-W Zhu, J. Tung, A. Phillips, G. Edward, Morphological development of oriented

430   isotactic polypropylene in the presence of a nucleating agent, Macromolecules 39

431   (2006) 1821-1831.

432   25. M. Liu, B. Guo, M. Du, F. Chen, D. Jia, Halloysite nanotubes as a novel β-nucleating

433   agent for isotactic polypropylene, Polymer 50 (2009) 3022-3030.

434   26. M. Kerscha, H.W. Schmidtb, V. Altstädta, Influence of different beta-nucleating agents

435   on the morphology of isotactic polypropylene and their toughening effectiveness,

436   Polymer 98 (2016) 320-326.

437   27. A. Romankiewicz, T. Sterzynski, W. Brostow, Structural characterization of α- and β-

438   nucleated isotactic polypropylene, Polym. Int. 53 (2004) 2086-2091.

439   28. Y.F. Zhang, X.X. Luo, L. Zhu, X.J. Yang, Y. Chang, Effects of α/β compound nucleating

440   agents on mechanical properties and crystallization behaviors of isotactic

441   polypropylene, J. Macromol. Sci. B. 51 (2012) 2352-2360.

442   29. P. Phulkerd, S. Arayachukeat, T. Huang, T. Inoue, S. Nobukawa, M. Yamaguchi,

443   Melting point elevation of isotactic polypropylene, J. Macromol. Sci. B. 53 (2014)

444   1222-1230.

445   30. Y. Uchiyama, S. Iwasaki, C. Ueoka, T. Fukui, K. Okamoto, M. Yamaguchi, Molecular

446   orientation and mechanical anisotropy of polypropylene sheet containing N,N-

447   dicyclohexyl-2,6-naphthalenedicarboxamide, J. Polym. Sci. B Polym. Phys. 47 (2009)

448   424-433.

449   31. M. Yamaguchi, T. Fukui, K. Okamoto, S. Sasaki, Y. Uchiyama, C. Ueoka, Anomalous

450   molecular orientation of isotactic polypropylene sheet containing N,N'-dicyclohexyl

451   2,6-naphthalenedicarboxamide, Polymer 50 (2009) 1497-1504.

452   32. M. Yamaguchi, Y. Irie, P. Phulkerd, H. Hagihara, S. Hirayama, S. Sasaki, Plywood-like

453   structure of injection-moulded polypropylene, Polymer 51 (2010) 5983-5989.

454   33. P. Phulkerd, S. Nobukawa, Y. Uchiyama, M. Yamaguchi, Anomalous mechanical

455   anisotropy of β form polypropylene sheet with *N,N'*-dicyclohexyl-2,6-naphthalene-

456   dicarboxamide, Polymer 52 (2011) 4867-4872.

457   34. P. Phulkerd, H. Hagihara, S. Nobukawa, Y. Uchiyama, M. Yamaguchi, Plastic

458   deformation behavior of polypropylene sheet with transversal orientation, J. Polym.

459   Sci. B Polym. Phys. 51 (2013) 897-906.

460   35. P. Phulkerd, S. Hirayama, S. Nobukawa, T. Inoue, M. Yamaguchi, Structure and

461   mechanical anisotropy of injection-molded polypropylene with a plywood structure,

462   Polym. J. 46 (2014) 226-233.

463   36. J. Varga, I. Mudra, G. W. Ehrensten, Highly active thermally stable β-nucleating agents

464   for isotactic polypropylene, J. Appl. Polym. Sci. 74 (1999) 2357-2368.

465   37. C. Grein, M. Gahleitner, On the influence of nucleation on the toughness of iPP/EPR

466   blends with different rubber molecular architectures, Express. Polym. Lett. 2 (2008)

467   392-397.

468   38. Y. Chen, S. Yang, H. Yang, M. Zhang, Q. Zhang, Z. Li, Toughness reinforcement in

469   carbon nanotube-filled high impact polypropylene copolymer with β-nucleating

470   agent, Ind. Eng. Chem. Res. 55 (2016) 8733-8742.

471   39. S. Sato, T. Maeda, M. Yamaguchi, Control of chain orientation in blends of

472   polypropylene and polybutene-1, Macromol. Mater. Eng. 302 (2017) 1600413-

473   1600421.

474   40. M. Takayanagi, K. Imada, T. Kajiyama, Mechanical properties and fine structure of

475   drawn polymers, J. Polym. Sci., Part C 15 (1967) 263-281.
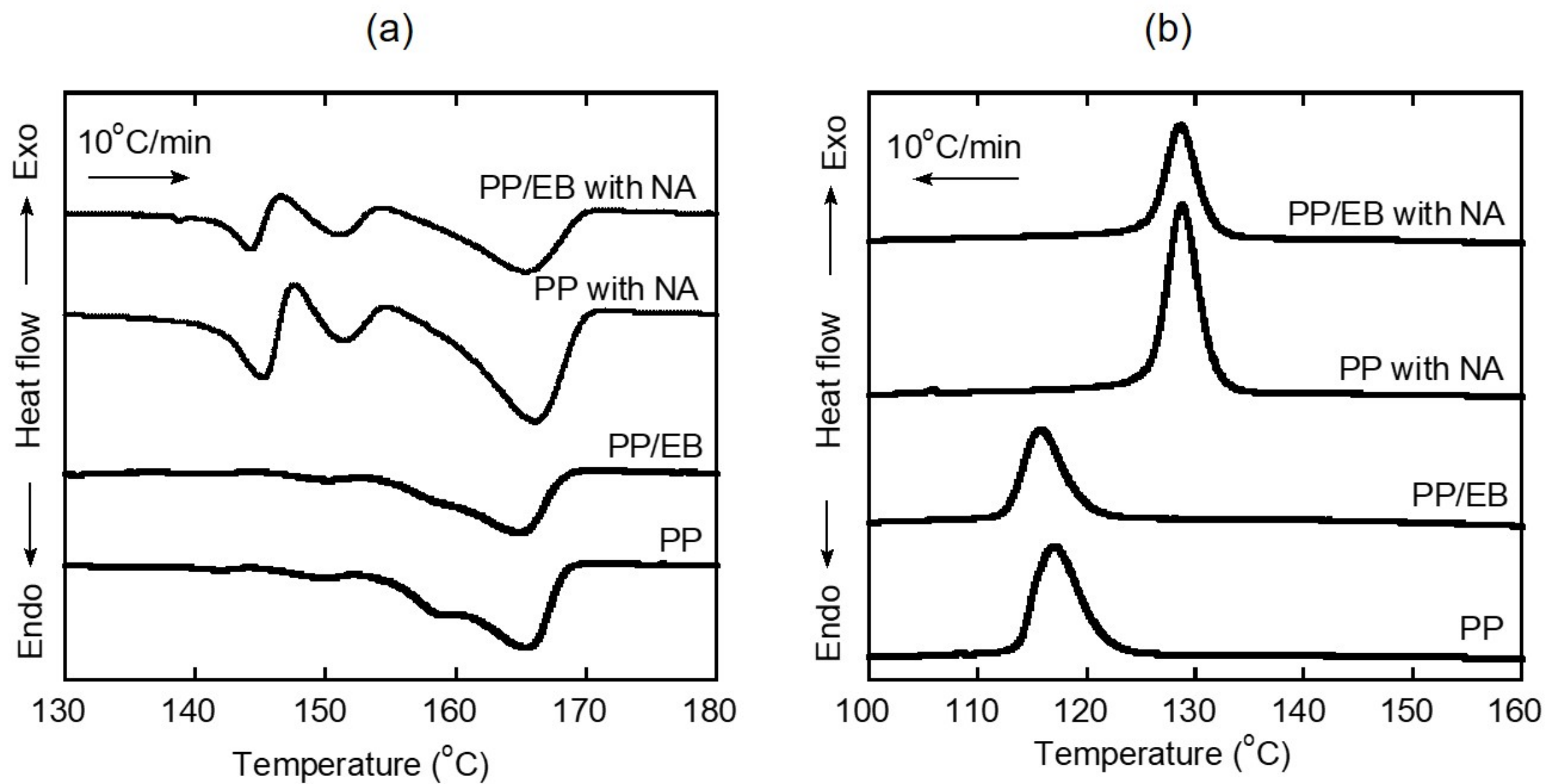
476

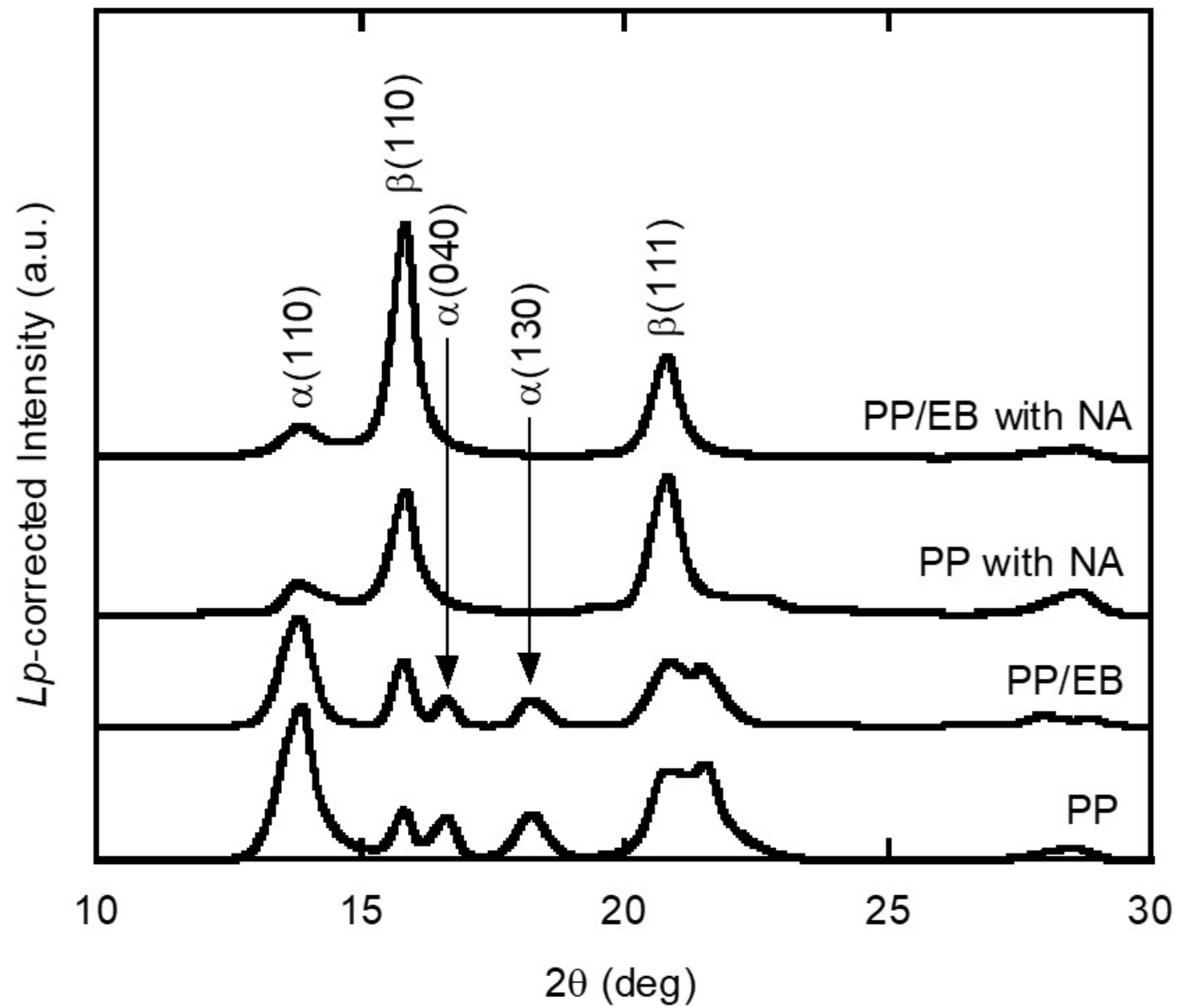Fig. 1 DSC profiles of extruded sheets; (a) heating curves and (b) cooling curves.

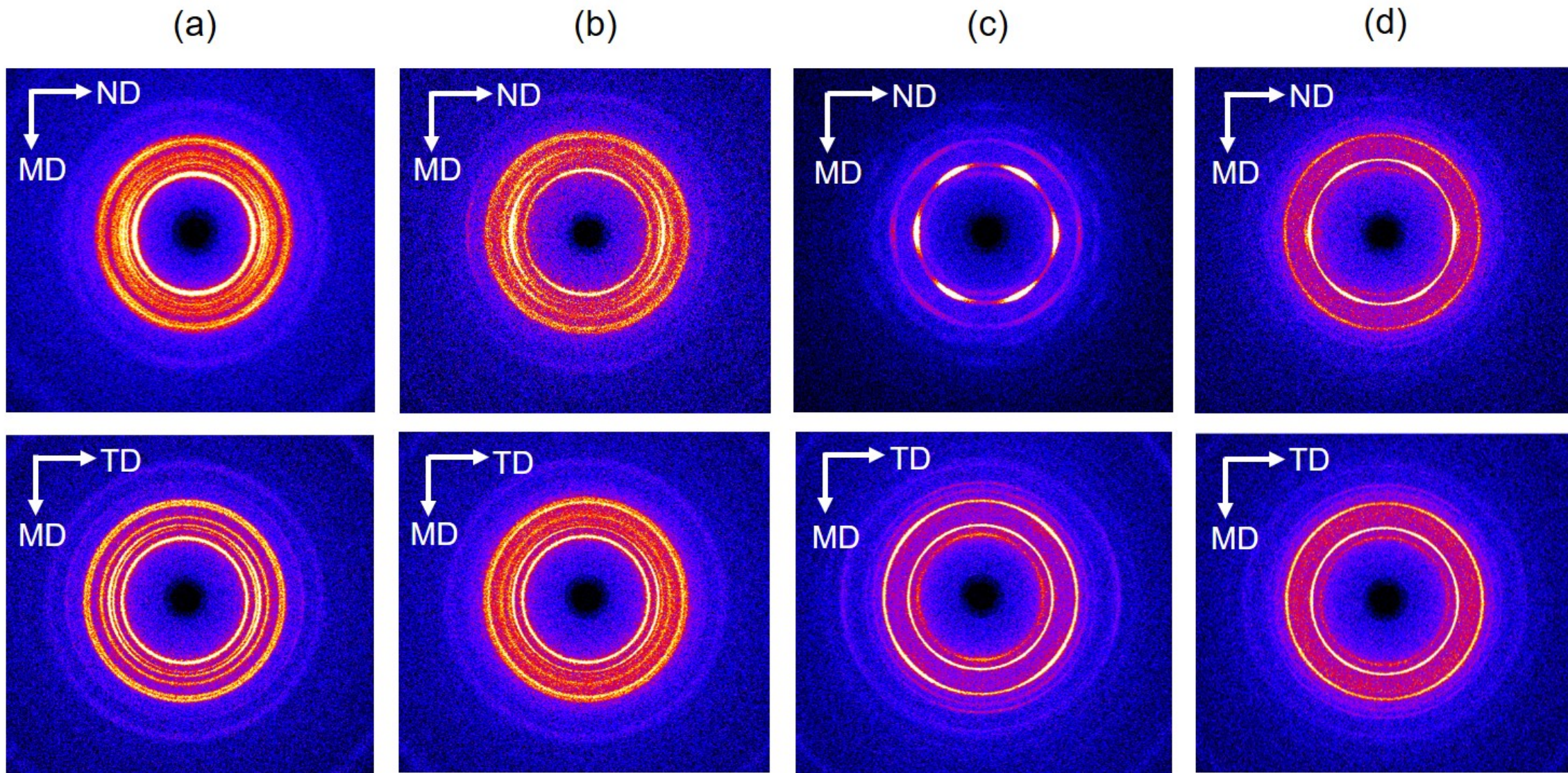Fig. 2 Lp-corrected XRD curves obtained from the through view beam for extruded sheets.

Fig. 3 WAXD patterns of the edge views (MD-ND) and the through views (MD-TD) in the samples; (a) PP, (b) PP/EB, (c) PP containing the nucleating agent, and (d) PP/EB containing the nucleating agent.
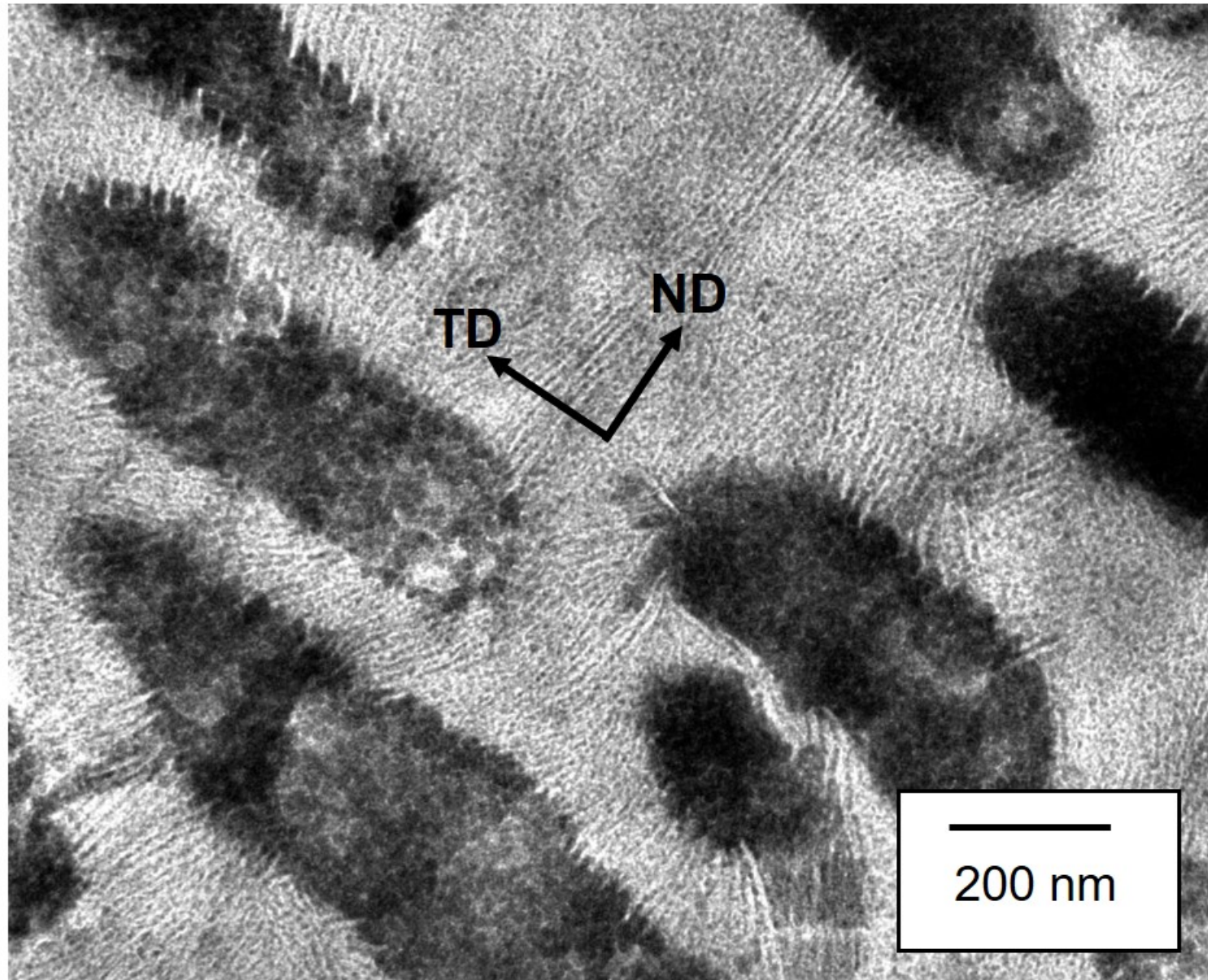
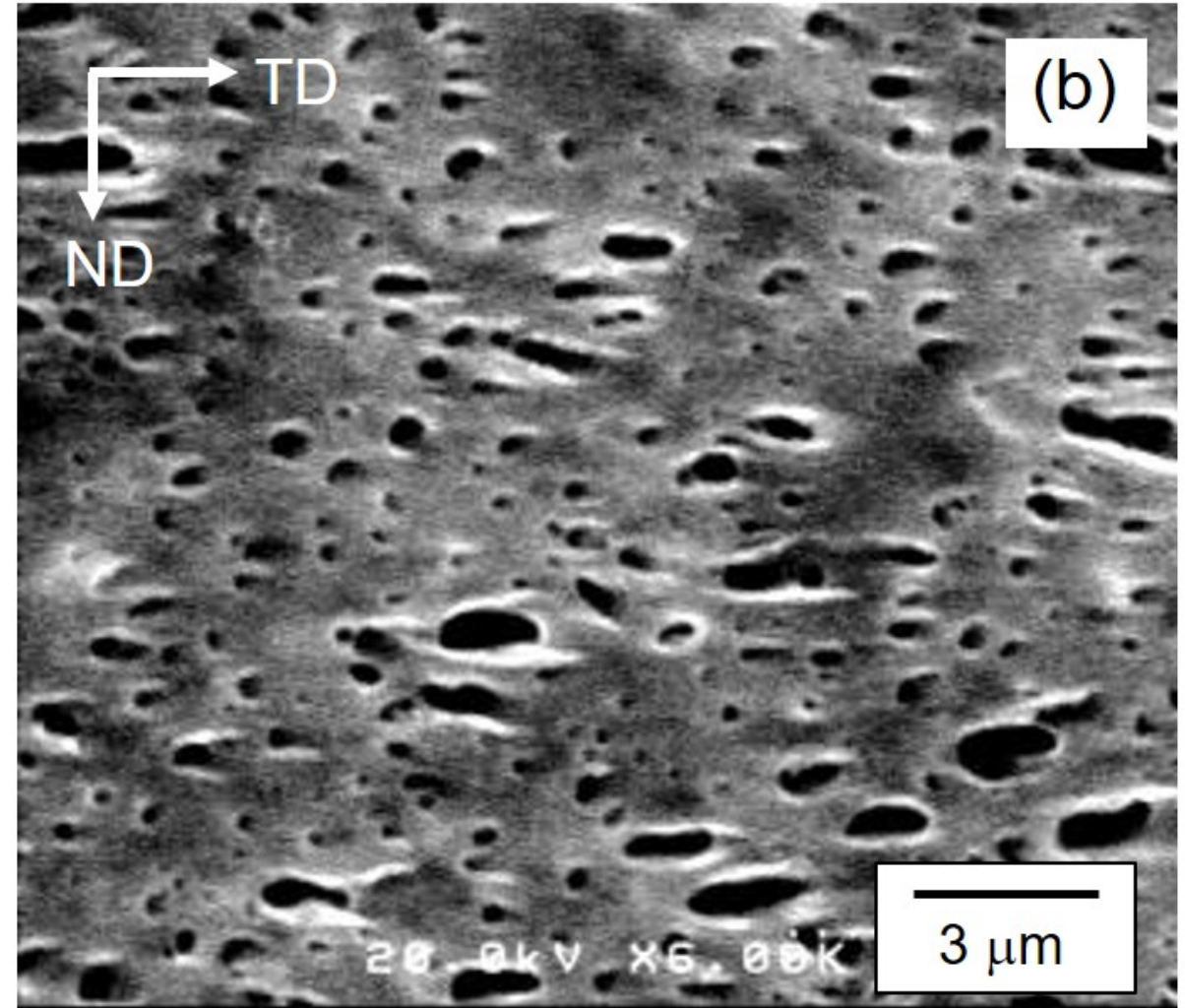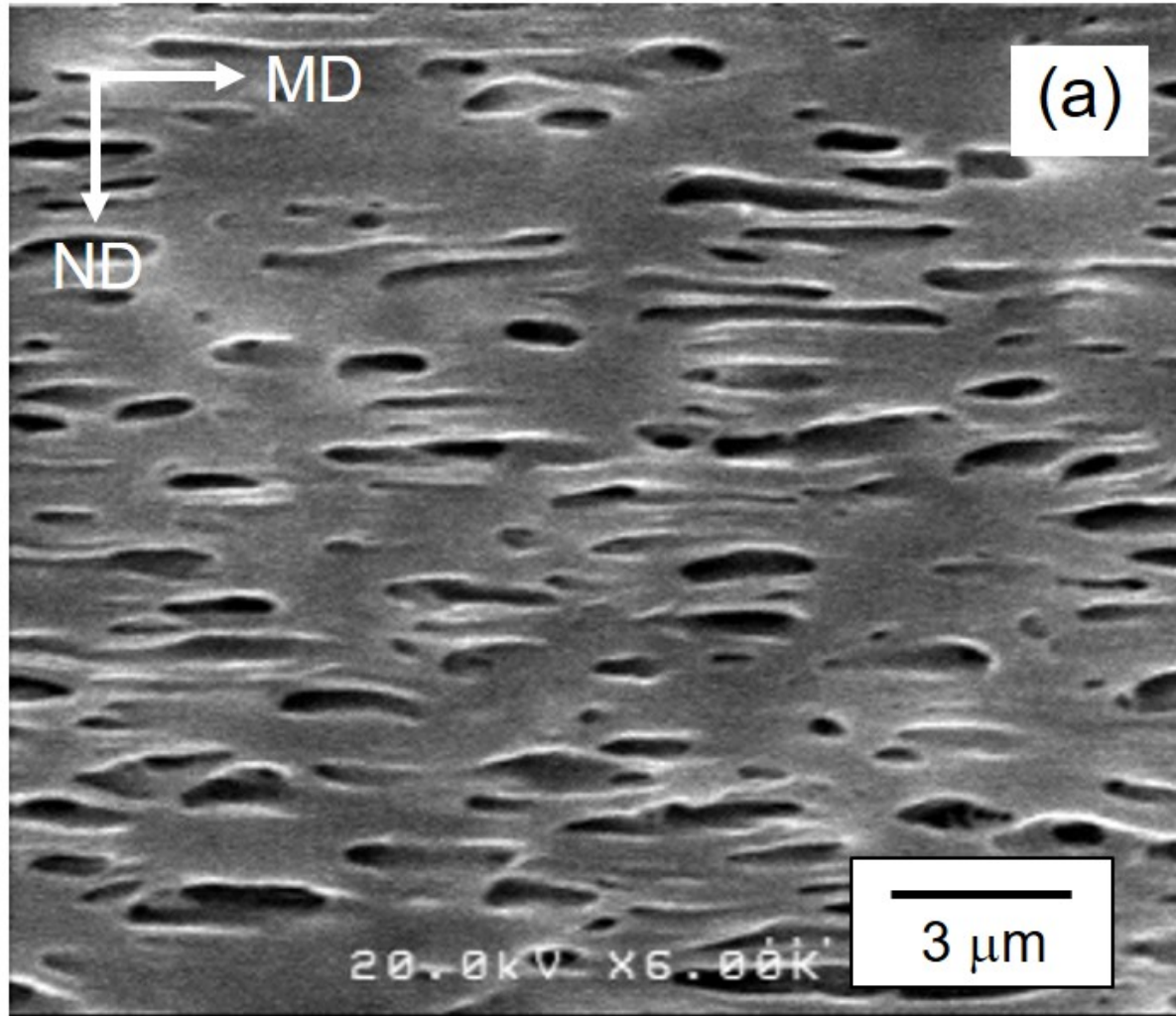Fig. 4 TEM image of the TD-ND plane (×15,000) for PP/EB containing the nucleating agent.

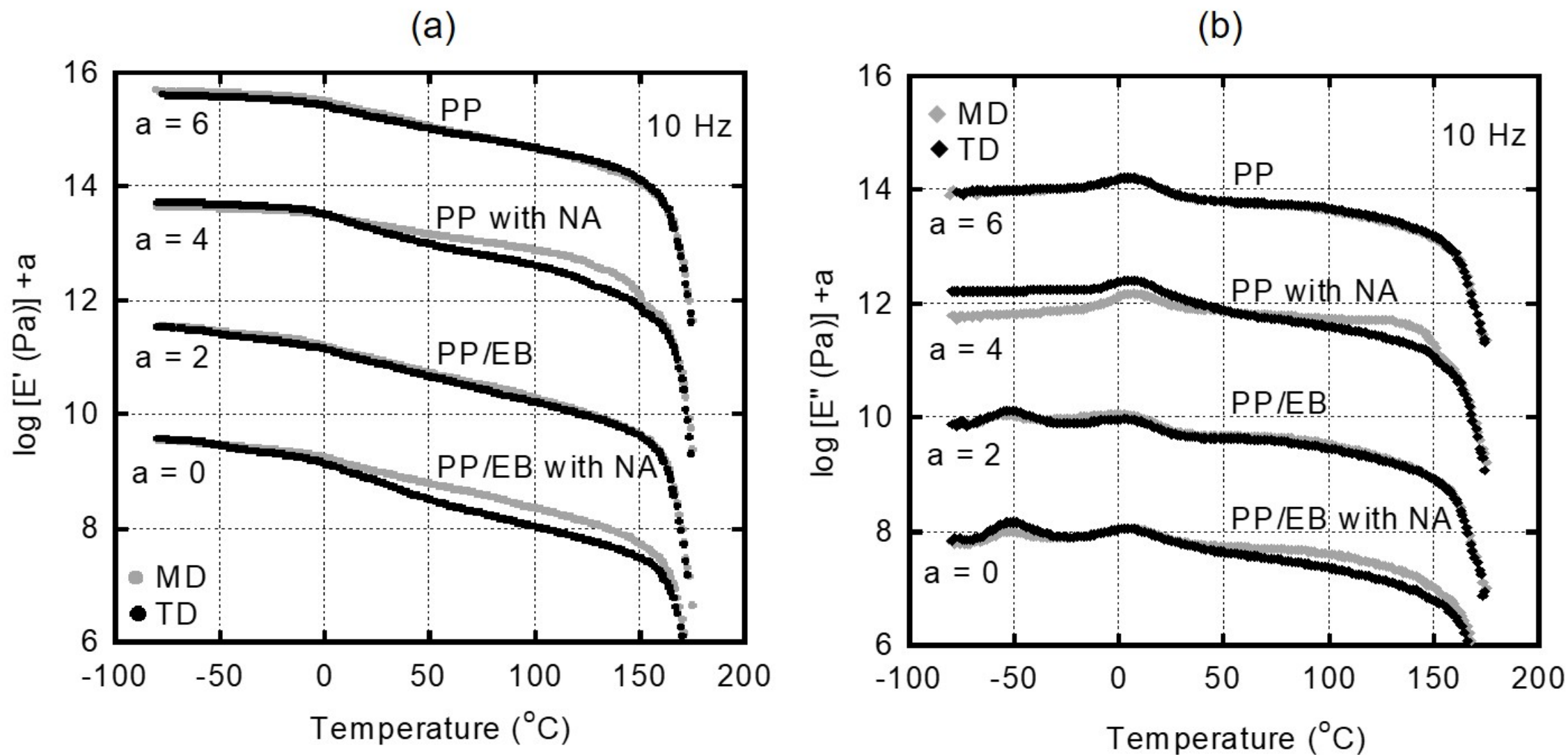Fig. 5 SEM images of PP/EB containing the nucleating agent. (a) MD-ND plane and (b) TD-ND plane.

Fig. 6 Temperature dependence of dynamic tensile modulus of extruded sheets at 10 Hz; (a) tensile storage modulus E' and (b) tensile loss modulus E''. The applied strain was (grey symbol) parallel to the flow direction (MD) and (black symbol) perpendicular to the flow direction (TD).
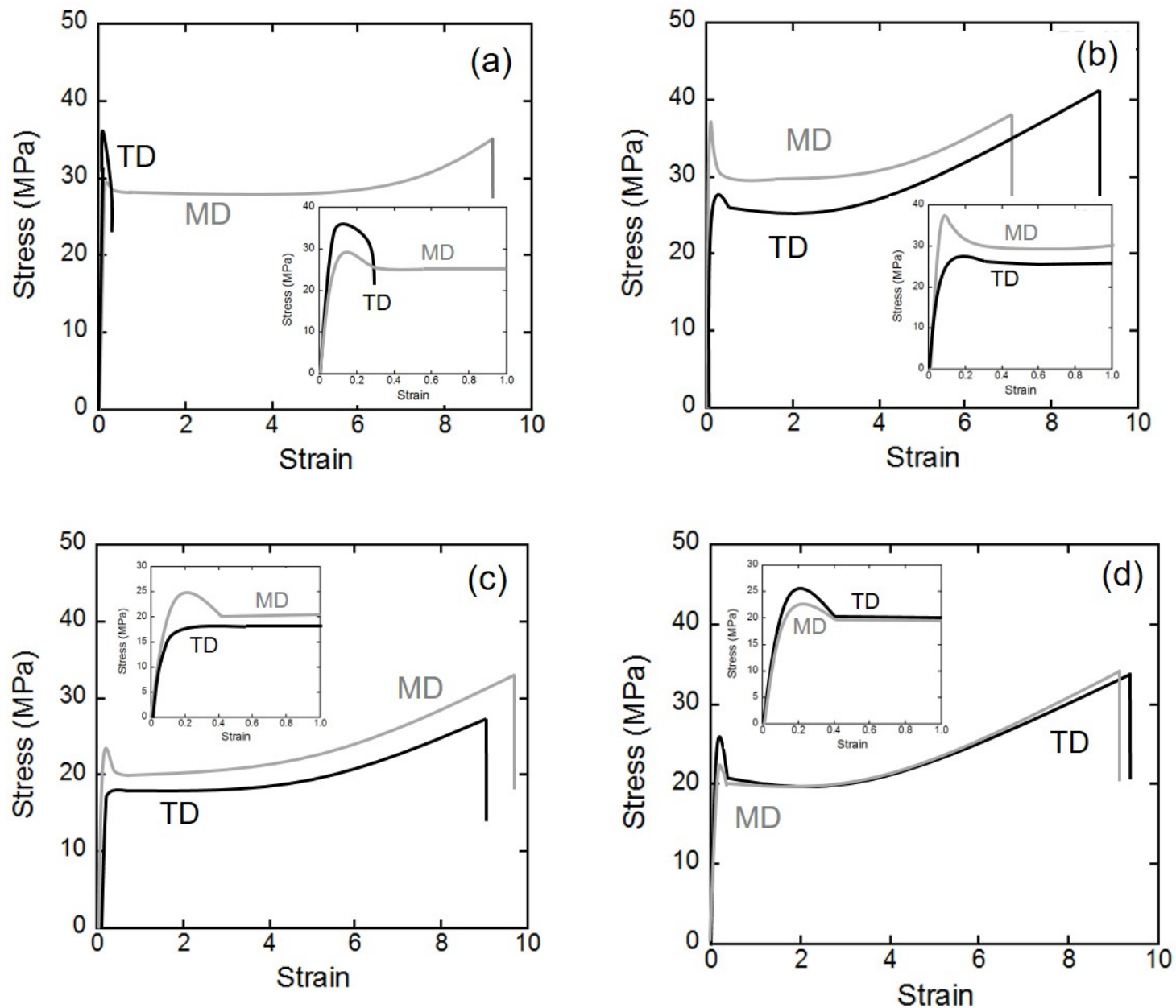
Fig. 7 Stress-strain curves of (a) PP, (b) PP containing the nucleating agent, (c) PP/EB, and (d) PP/EB containing the nucleating agent at a strain rate of $0.006 \, s^{-1}$.
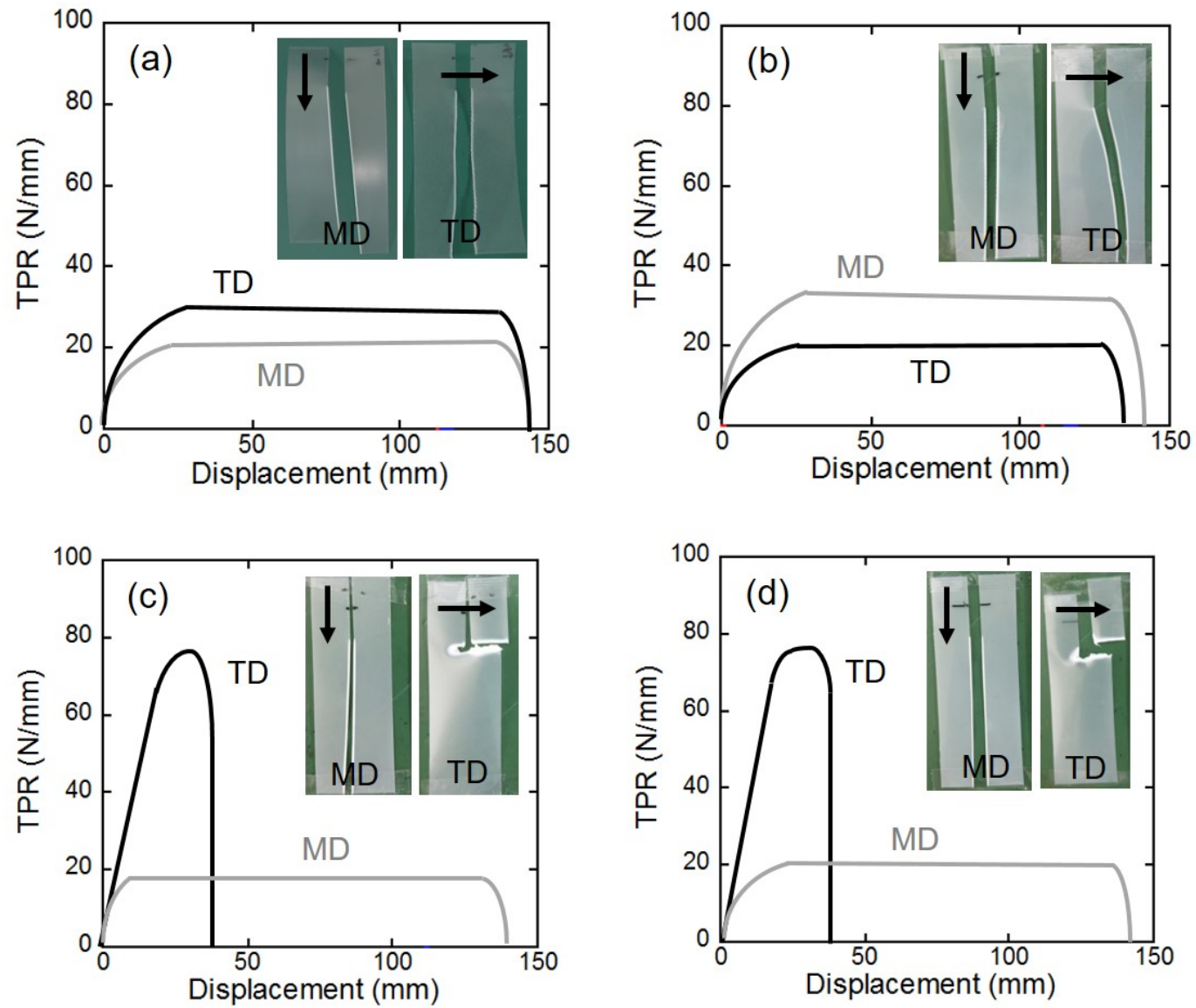
Fig. 8 Tear-propagation resistance (TPR) versus the applied displacement of notched specimens in MD and TD directions; (a) PP, (b) PP containing the nucleating agent, (c) PP/EB, and (d) PP/EB containing the nucleating agent.